Preparation of Magnetic Poly(glycidyl methacrylate) Microspheres by Emulsion Polymerization in the Presence of Sterically Stabilized Iron Oxide Nanoparticles

Daniel Horák, Nataliya Chekina

Institute of Macromolecular Chemistry, Academy of Sciences of the Czech Republic, Prague 6, Czech Republic

Received 29 August 2005; accepted 3 June 2006
DOI 10.1002/app.24923
Published online in Wiley InterScience (www.interscience.wiley.com).

ABSTRACT: With the aim to synthesize water-dispersible superparamagnetic nanoparticles, iron oxide was precipitated in aqueous solution of dextran, (carboxymethyl)-dextran (CM-dextran), (DEAE-dextran), or D-mannose. Glycidyl methacrylate (GMA) was emulsion-polymerized in the presence of the nanoparticles and the effect of iron oxide modification on the product properties was investigated. The main factors affecting the morphology, size, and size distribution of the latex particles are the type and concentration of emulsifier (Disponil AES 60, Tween 20, Triton X-100) and initiator [ammonium persulfate (APS) and 4,4′-azobis(4-cyanovaleric acid) (ACVA)]. Disponil AES 60 and ACVA are the preferred emulsifier and initiator, respectively, because oxirane groups hydrolyzed during the APS-initiated polymerization. Up to some 5 wt % of iron was found in poly(-glycidyl methacrylate) (PGMA) microspheres obtained by emulsion polymerization in the presence of dextran-coated iron oxide and emulsified with Disponil AES 60. The size of magnetic PGMA microspheres could be controlled in the range ~ 70–400 nm. © 2006 Wiley Periodicals, Inc. J Appl Polym Sci 102: 4348–4357, 2006

Key words: iron oxide; emulsion polymerization; glycidyl methacrylate; Disponil AES 60

INTRODUCTION

Magnetic polymer nano- and microspheres are an area of great interest because the combination of easily modifiable polymer support and its responsiveness to a magnetic field greatly enhances possibilities of its easy manipulation, separation, and targeting. Recently developed magnetic nanoparticles can be used in data storage applications[1] (if they are not affected by temperature fluctuations), catalysis, and biomedical applications.[2,3] All biomedical applications require that the nanoparticles should be water-dispersible and superparamagnetic and the overall size distribution should be narrow. Biomedical applications can be classified into *in vivo* applications which could be further separated in therapeutic (hyperthermia and drug- or gene-targeting)[4] and diagnostic applications (enhancing the image contrast between normal and damaged tissue, indicating organ functions or blood flow by NMR imaging),[5] while for *in vitro* applications the main use is in diagnostic (separation/selection,[6] and magnetorelaxometry[7]). In *in vivo* applications, the particles may be injected intravenously or directly into the area where treatment is desired. Beneficial factors of small particles include a large surface-to-volume ratio facilitating attachment of ligands. The application of magnetic nanoparticles *in vivo* requires their surface modification by coating with a nontoxic, nonimmunogenic and biocompatible polymer during or after the synthesis. It prevents the formation of large aggregates and ensures stability to the reticuloendothelial system. Nanoparticles are often made of iron oxide, in particular magnetite, which is biocompatible, and thus has an advantage over highly magnetic materials such as cobalt and nickel, which are toxic and susceptible to oxidation. The method of preparation of core magnetic particles determines the particle size and shape, size distribution, the surface chemistry of the particles, and, consequently, their magnetic properties. Magnetic materials have irregular shape when obtained by grinding bulk materials but can have a spherical shape when prepared by wet chemistry[8] or decomposition of metal carbonyl complexes. Depending on the mechanism of formation, spherical particles can be amorphous or crystalline. The colloidal stability depends primarily on the dimensions of the particles, which should be sufficiently small so that precipitation or sedimentation due to gravitation forces can be avoided and also on the charge and surface chemistry (steric and electrostatic Coulombic repulsions).

Encapsulation of magnetite nanoparticles into organic polymer microspheres renders the microspheres magnetic. Polymer coatings on particles enhance compatibility with organic ingredients and reduce susceptibility to leaching. Encapsulation improves dispersibility, chemical stability, and reduces toxicity. Successful

Correspondence to: D. Horák (horak@imc.cas.cz).
Contract grant sponsor: Grant Agency of the Czech Republic; contract grant number: 203/05/2256.

© 2006 Wiley Periodicals, Inc.

encapsulation, however, requires a good dispersion of inorganic particles in the medium prior to polymerization.

In an attempt to develop monodisperse magnetic polymer microspheres with uniform physical and chemical properties[9] and containing reactive functional groups for attachment of biomolecules, this report focuses on emulsion polymerization of glycidyl methacrylate in the presence of sterically stabilized magnetic nanoparticles. Preparation of magnetic styrene and methyl methacrylate latices by emulsion polymerization was already studied by Noguchi;[10] the mechanism of emulsion polymerization is well known.[11] The advantage of emulsion, in contrast to, e.g., dispersion polymerization, consists in the presence of an emulsifier capable of contributing to stabilization of iron oxide. Of other methods to produce magnetic latex particles, multistep swelling and polymerization,[12] miniemulsion polymerization,[13] and suspension polymerization[14] can be exemplified. Some of them were recently reviewed.[15] Such polymer/inorganic composite (hybrid) materials possessing excellent properties with synergistic effect could find applications in many fields, such as separation of biomolecules from complex mixtures or for the detection of pathogens in food.

EXPERIMENTAL

Chloroacetic acid was obtained from Lachema Neratovice (Czech Republic), dextran T 40 (M_w = 33,000; M_w/M_n = 1.4) from Dextran Products (Scarborough, Canada), DEAE-dextran from Sigma, and Disponil AES 60 [(sodium poly(oxyethylene) alkylaryl ether sulfate)] from Henkel. D-Mannose, Tween 20 [poly-(oxyethylene) sorbitan monolaurate], and Triton X-100 [(poly(oxyethylene) isooctyl phenyl ether)] were purchased from Fluka, 4,4′-azobis(4-cyanovaleric acid) (ACVA), ammonium persulfate (APS), MES (2-morpholinoethanesulfonic acid), and other chemicals from Aldrich and were used as received.

Synthesis of (carboxymethyl)dextran[16] (CM-dextran)

Dextran T 40 (20 g) was dissolved in 283 mL of *tert*-butyl alcohol, then 50 mL of 3.8*M* NaOH was slowly added and the mixture stirred for 1 h at laboratory temperature. Chloroacetic acid (50 g; 2.5*M* excess to dextran) was added and the mixture was heated to 60°C for 90 min, and then neutralized with glacial acetic acid. The product (white powder) was precipitated from methanol, filtered off, washed with methanol, and vacuum-dried at 40°C for 2 h. The product contained 3.5 mmol carboxyl groups per gram as determined by titration (degree of substitution 0.79).

Synthesis of dextran (No. 1)-, (carboxymethyl) dextran (No. 2)-, [2-(diethylamino)ethyl]dextran (No. 3)-, and D-mannose (No. 4)-coated iron oxide[17]

About 10 mL of 50 wt % CM-dextran (or dextran or D-mannose) or aqueous solution of 25 wt % of [2-(diethylamino)ethyl]dextran (it was difficult to precipitate iron oxide in 50 wt % solution) was mixed under stirring with 10 mL of aqueous solution of 1.51 g $FeCl_3 \cdot 6H_2O$ and 0.64 g $FeCl_2 \cdot 4H_2O$. About 15 mL of 7.5% NH_4OH solution was dropwisely added until the pH reached 12 and the mixture was heated to 60°C for 15 min. Large aggregates were destroyed by sonication (W 385 Sonicator; Cole-Palmer Instruments, USA; output 40%) for 5 min. To remove unreacted iron salts, the product was washed by dialysis against water, using molecular weight cut-off 14,000 Visking membrane (Carl Roth GmbH, Germany), for 24 h at room temperature, changing water 5 times (2 L each time) until the pH reached 6. The volume was reduced by evaporation: the resulting colloid contained 80 mg iron oxide/mL.

Emulsion polymerization of GMA

The following experiment serves as an example. A 100-mL reactor was loaded with 47.5 mL water, 12.5 mL of ferrofluid containing 1 g iron oxide, 0.9 g Disponil AES 60, 9 g GMA, and 0.18 g APS or ACVA in 1.5 mL 1*M* NaOH. The reaction mixture was bubbled with nitrogen for 10 min and polymerized under stirring (500 rpm) at 70°C for 20 h. All products were purified by dialysis (Visking membrane, molecular weight cut-off 14,000) and at least two cycles of ultracentrifugation (Beckman model L8-55, rotor SW 27; 5 h at 15,000 rpm), decantation, and redispersion in water. The particles were then magnetically responsive. Finally, the microspheres were freeze-dried.

Characterization

Transmission electron microscopy (TEM) was performed on a JEOL JEM 200 CX to determine particle size of ferrofluids. Polymer particles were observed in a scanning electron microscope (SEM, JEOL JSM 6400), and the size and polydispersity (PDI = D_w/D_n, where D_w and D_n is weight- and number-average particle diameter, respectively) were determined from the photographs (at least 500 particles) using image analysis software Atlas (Tescan, Brno, Czech Republic). A Perkin–Elmer FTIR spectrometer Paragon 1000PC was used both to confirm the presence of carboxymethyl group in CM-dextran and to determine the oxirane group content in PGMA microspheres (on the basis of the peak area at 910 cm^{-1}). Data scatter in the determination reached up to 20% due to the sample inhomogeneity. A titrator 799 GPT Titrino (Metrohm) was used to evaluate the content of carboxyl groups in

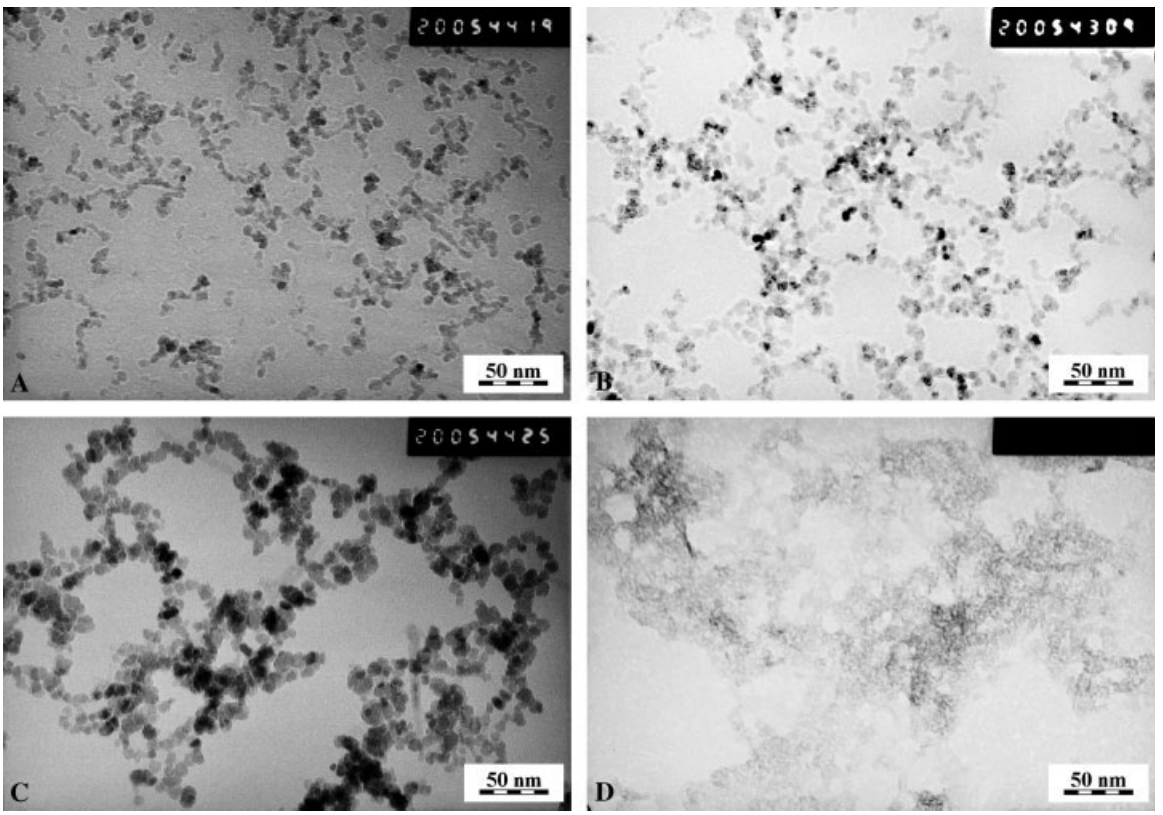

Figure 1 TEM of (a) dextran (No. 1), (b) (carboxymethyl)dextran (No. 2), (c) [2-(diethylamino)ethyl]dextran (No. 3), and (d) D-mannose (No. 4) stabilized iron oxide nanoparticles.

CM-dextran. The amount of iron in the particles was analyzed by AAS (Perkin–Elmer 3110) of an extract from the sample obtained with dilute HCl (1 : 1) at 80°C for 1 h.

RESULTS AND DISCUSSION

Preparation of iron oxide

The properties of finely divided magnetic materials closely depend on the size of the particles and their state of dispersion and aggregation.[18] The formation of mixed ferric–ferrous phases depends on many factors such as the iron concentration, pH, and, in particular, the system composition (Fe^{3+}/Fe^{2+} ratio). Iron oxide was synthesized in one-step process by alkaline coprecipitation of iron(II) and iron(III) precursors in aqueous solution of hydrophilic compounds. Four saccharides, namely dextran, CM-dextran, DEAE-dextran, and D-mannose, were compared as iron oxide coatings. CM-dextran was obtained by the reaction of dextran with chloroacetic acid. The presence of COOH groups in (carboxymethyl)dextran was confirmed by the 1608 cm^{-1} band in IR spectrum. The role of these compounds is the limitation of the magnetic core growth during the synthesis, their steric stabilization in water, and *in vivo* reduction of the opsonization process (susceptibility to the action of phagocytes).[19] Steric stabilization provides entropic repulsion needed to overcome the short-range van der Waals attraction that otherwise results in irreversible particle aggregation.

First, dextran, the hydroxy groups of which are known to enable polar interactions (mainly chelation and H-bonding) with iron oxide surface,[20] was tested as a coating. The TEM image of iron oxide nanoparticles was used to determine the shape and size of the particles. The advantage of TEM, in contrast to other methods (e.g., light scattering), is that one can decide what belongs in the micrograph to the particle system and what not; artifacts can be thus eliminated. Even when the particles were not strictly spherical, they were isometric and could be approximated by spheres for the purpose of the particle size determination by image analysis. Figure 1(a) shows dextran-stabilized iron oxide nanoparticles No. 1 $\sim$ 4 nm in size forming aggregates with the size up to 10 nm. Dextran renders the magnetic nanoparticles biocompatible and thus makes this method especially appropriate for *in vivo* applications. A high amount of dextran seems to remain in the product after the dialysis as the nanoparticles contained only less than 20 wt % of iron (Table I).

Second, (carboxymethyl)dextran (CM-dextran) was used as a coating to stabilize iron oxide and to

TABLE I
Characterization of Coated Iron Oxide Nanoparticles

No.	Coating	Fe content (wt %)	D_n (nm)	Concentration (g iron oxide/mL)
1	Dextran	17.8	4	0.08
2	CM-dextran	19.1	5	0.06
3	DEAE-dextran	29.0	6	0.06
4	D-Mannose	50.1	2	0.02

compare its properties with those of dextran-stabilized iron oxide. CM-dextran was chosen because of the well-known affinity of the COOH groups to Fe^{2+} ions.[21] The dextran part then allows the dispersion in water and prevents aggregation of the particles forming a stable colloid. Colloidal iron oxide precipitated in the presence of (carboxymethyl)dextran (No. 2) formed ''chains'' of fine particles $\sim$ 5 nm in diameter [Fig. 1(b)]. To see the effect not only of negative, but also that of positive charge on the nanoparticle properties, DEAE-dextran was also tested as an iron oxide coating. DEAE-dextran-coated iron oxide nanospheres No. 3 [Fig. 1(c)] were slightly larger than that of the dextran- or CM-dextran-coated ones (TEM observation), with diameter $\sim$ 6 nm. An interesting situation was observed with low molecular weight saccharide-stabilized iron oxide No. 4. D-Mannose was selected for this purpose as it is known to have important biological properties.[22] According to TEM, an extremely small particle size was obtained after coprecipitation in the presence of D-mannose [Fig. 1(d)]—nanoparticles had size about 2 nm, with a tendency to aggregate. Besides iron oxide nanoparticles, a discontinuous D-mannose film can be observed in Figure 1(d). An inverse proportionality between polysaccharide molecular weight and particle size is in accordance with that of the literature data.[8]

Emulsion polymerization in the presence of colloidal iron oxide

In our previous reports, magnetic poly(2-hydroxyethyl methacrylate) or poly(glycidyl methacrylate) microspheres were prepared by dispersion polymerization in the presence of various magnetic seeds.[23–25] In this report, emulsion polymerization of GMA was carried out in the presence of four ferrofluids using APS or 4,4′-azobis(4-cyanovaleric acid) as an initiator. In emulsion polymerization, the surfactant plays an

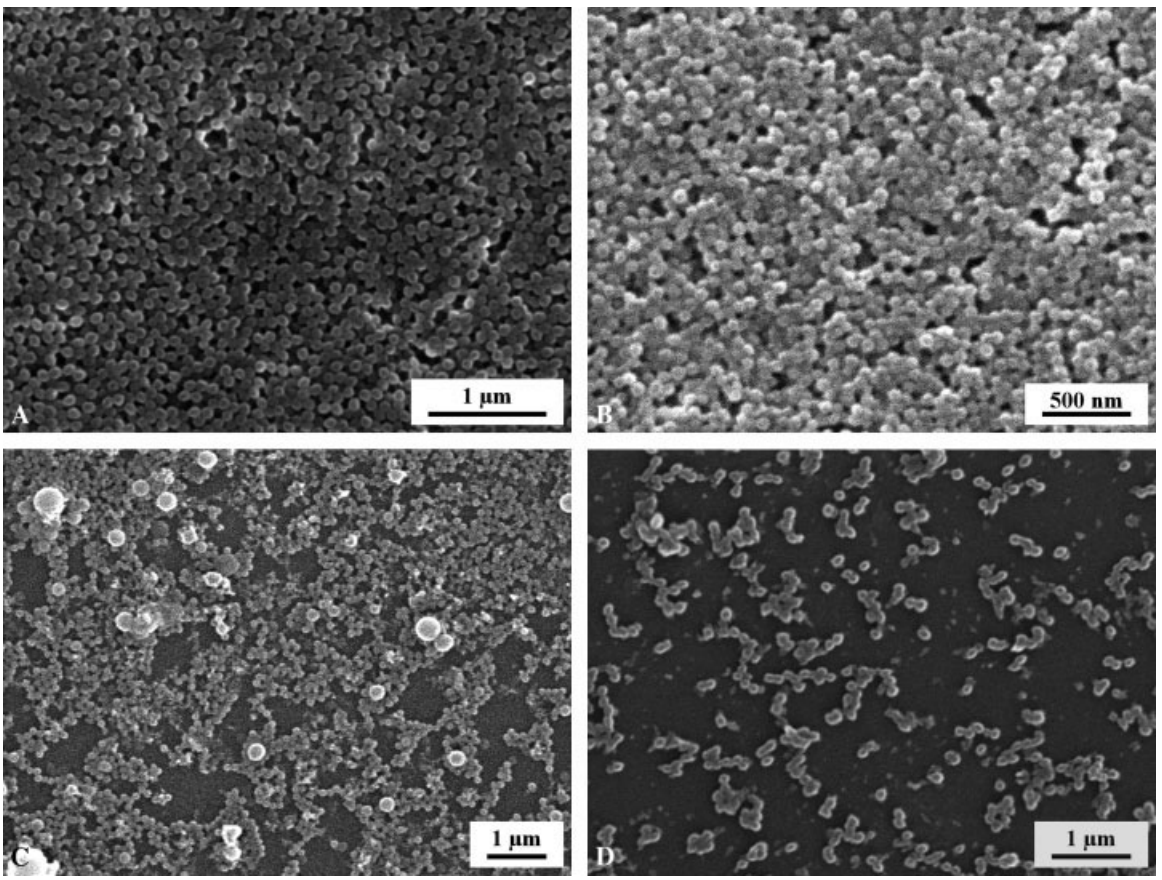

Figure 2 SEM of magnetic PGMA microspheres obtained at (a) dextran-coated, (b) CM-dextran-coated, (c) DEAE-dextran-coated, and (d) D-mannose-coated iron oxide/GMA weight ratio 0.33. Polymerization conditions: 0.26 wt % ACVA (relative to feed); (a) 0.38 and (b–d) 1.5 wt % Disponil AES 60 in water.

important role in the stability, rheology, and control of the particle size of the resulting latices. Disponil AES 60, Tween 20, and Triton X-100 were the surfactants used in this study. The resulting PGMA microspheres were black and clearly showed magnetic behavior in the magnetic field. The thoroughly washed particles were characterized by SEM to see the particle shape, size, morphology, and aggregation. Under the given conditions, it is difficult to asses from the SEM micrographs whether the iron oxide nanoparticles were localized on the surface or incorporated in the latex particles [Figs. 2(a–d)]. No free iron oxide was discernible with the exception of D-mannose-stabilized ferrofluid at the iron oxide/GMA ratio 0.33. This is in contrast to the dispersion polymerization, where a part of the iron oxide particles could not be incorporated in the latex particles[26] if the iron oxide/GMA weight ratio in the feed exceeded 0.05. The mechanism of the present emulsion polymerization in the presence of iron oxide nanoparticles is much more complex than that of ordinary emulsion polymerization. Nevertheless, we suppose that hydrophilic sulfate or carboxyl groups present in the polymer chains from the APS or ACVA initiator, respectively, might facilitate compatibilization of PGMA with hydrophilic saccharide-coated iron oxide.

As confirmed by SEM micrographs (Fig. 2), latex particles obtained under ACVA initiation preserved their discrete spherical shape and no marked aggregation of the latex particles occurred. PGMA microspheres, however, differed both in size and polydispersity depending on the type of iron oxide coating. While the microspheres obtained in the presence of dextran- and CM-dextran-coated iron oxide were alike, those resulting from DEAE-dextran- and D-mannose-coated iron oxide added to the polymerization feed were different. Typical SEM micrograph of PGMA microspheres obtained with dextran-coated iron oxide showed particles with a size of 95 nm and narrow size distribution characterized by PDI = 1.02 [Fig. 2(a)]. Similarly, size of PGMA microspheres containing CM-dextran-coated iron oxide [shown in Fig. 2(b)] was $\sim$ 75 nm; the particle size distribution was also narrow (PDI = 1.04). In contrast, PGMA microspheres obtained in the presence of DEAE-dextran-coated iron oxide were substantially inferior to those obtained in the presence of dextran- or CM-dextran-coated nanoparticles. Two kinds of particles, namely white nonmagnetic and magnetic PGMA microspheres, were formed in the polymerization in the presence of DEAE-dextran-coated iron oxide. Nonmagnetic particles were removed by decantation. As a consequence, magnetic particles contained high amounts of iron oxide ($\sim$ 9–15 wt % when DEAE-dextran-coated iron oxide/GMA ratio ranged 0.1–0.3), compared with PGMA microspheres prepared in the presence of dextran- or CM-dextran-coated iron oxide (Fig. 3). Larger (160 nm) microspheres than in the previous set of experiments were obtained with DEAE-dextran-coated iron oxide in the polymerization feed [Fig. 2(c)]. Moreover, the microspheres were polydisperse (PDI = 1.73). A typical SEM micrograph of PGMA microspheres obtained in the presence of D-mannose-stabilized iron oxide showed not strictly spherical particles $\sim$ 130 nm in size with a narrower particle size distribution [Fig. 2(d); PDI = 1.04]. However, some very fine nonencapsulated iron oxide particles were also present in the product. Similarly, like with PGMA microspheres containing DEAE-dextran-coated iron oxide, relatively high iron content in the particles prepared in the presence of D-mannose-coated iron oxide (Fig. 3) can be ascribed to the presence of bare iron oxide nanoparticles.

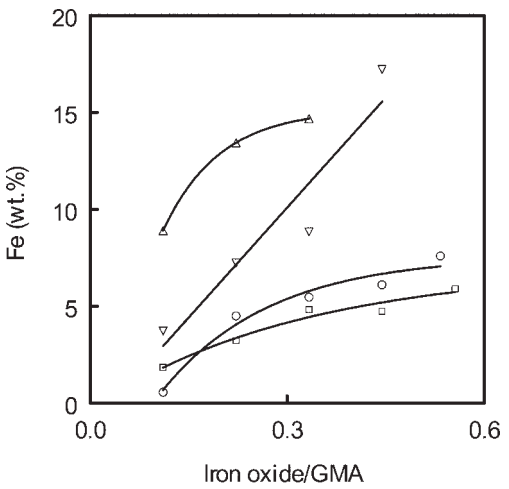

Figure 3 Dependence of the iron content in magnetic PGMA microspheres on iron oxide/GMA weight ratio. Iron oxide coated with (□) dextran, (△) DEAE-dextran, (○) CM-dextran, and (▽) D-mannose. Polymerization conditions: 0.26 wt % of ACVA (relative to feed), 1.5 wt % Disponil AES 60 in water.

Effect of iron oxide to GMA weight ratio

To respond quickly to magnetic field, it is desirable to prepare magnetic microspheres with high iron oxide content. Only a limited amount of ferrofluid, however, can be added to the emulsion polymerization feed if narrow particle size distributions are to be obtained, which restricts the iron content in the microspheres. While the weight ratio of dextran- or CM-dextran-coated iron oxide to GMA up to 0.55 did not cause any noticeable problems, DEAE-dextran-coated iron oxide did not produce magnetic PGMA microspheres of the desired quality and incomplete incorporation of D-mannose-stabilized iron oxide was observed already at the weight ratio 0.33. As expected, the content of iron oxide incorporated in PGMA microspheres increased with increasing amount of

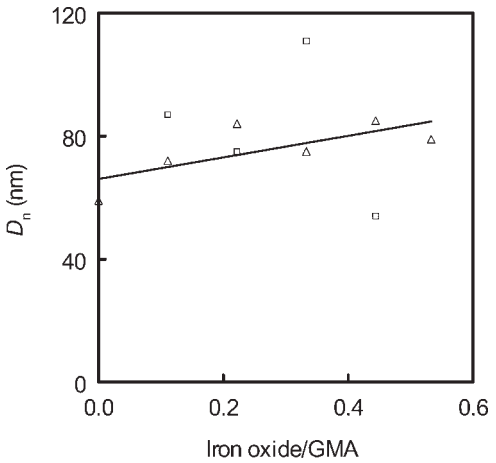

Figure 4 Effect of the weight ratio of iron oxide/GMA on the PGMA microsphere size D_n. Polymerization conditions: 15 wt % GMA (relative to water); 0.26 wt % (△) ACVA and (□) APS initiator in the feed; 1.5 wt % Disponil AES 60 in water; CM-dextran-coated iron oxide; total volume 70 mL; temperature 70°C; reaction time 20 h.

dextran-, CM-dextran-, DEAE-dextran, and D-mannose-containing ferrofluid in the polymerization feed (Fig. 3). It can be thus concluded that iron oxide content in the latex particles was primarily determined by the weight ratio of ferrofluid to monomer. Figure 4 illustrates the effect of CM-dextran-coated iron oxide to GMA weight ratio on the microsphere size. Nonmagnetic PGMA microspheres (prepared without the addition of ferrofluid in the feed) were rather small (around 60 nm) if Disponil AES 60 was used as emulsifier [Fig. 5(a)]; in contrast, Triton X-100 produced surprisingly large particles [1.1 μm; Fig. 5(b)]. This statement is extended also to magnetic microspheres (see below). Magnetic PGMA microspheres obtained under ACVA initiation and Disponil AES 60 emulsification were slightly larger than their nonmagnetic counterparts and their size increased with increasing iron oxide/GMA ratio (Fig. 4). This can be probably explained by inhibition of polymerization, as it is generally accepted that Fe^{2+} acts as a radical scavenger.[27] Fe^{2+} can thus promote the radical "wasting" and hence decrease the polymerization rate. As a result, molecular weight of polymer is low and particles stick together. Retardation of polymerization due to iron oxide was observed also by other authors.[28] The effect of increasing amount of iron oxide added to the polymerization mixture initiated by APS on the resulting particle size was not conclusive (Fig. 4).

Effect of initiator concentration

In this set of experiments on emulsion polymerization of GMA in the presence of dextran-coated iron oxide nanoparticles, the initiator type and its concentration in the feed were varied. As emulsion polymerization requires water-soluble initiators, APS was tested first. However, rather low contents of oxirane groups were produced under APS initiation due to their hydrolysis during the polymerization (see later). Therefore, the azo initiator ACVA, which introduces carboxyl groups into the microspheres, was employed. Although ACVA is water-insoluble, it dissolves in alkaline medium. ACVA was found to be superior to APS initiator, as the latter produced rather irregular particles. While with increasing APS concentration the PGMA diameter decreased, the dependence of microsphere size on ACVA concentration was not conclusive (Table II). The finding that smaller PGMA microspheres formed with increasing APS concentration favors the homogeneous nucleation mechanism proposed by Fitch and Tsai[29] supports the view that the coagulation nucleation mechanism is not the size-determining process. Presumably, even at high initiator concentrations, precursor particles are sufficiently stabilized by the ionized groups on the particle surface originating from the initiator. Similar observations were made by other authors.[30] Higher amounts

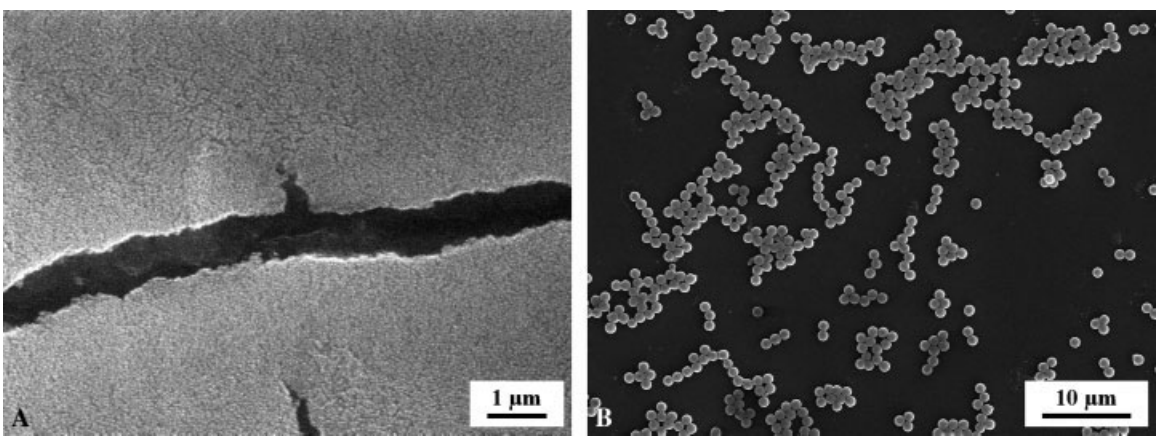

Figure 5 SEM of nonmagnetic PGMA microspheres obtained by emulsion polymerization with 1.5 wt % of (a) Disponil AES 60 and (b) Triton X-100 in water. 0.26 wt % ACVA in the feed.

TABLE II
Effect of APS and ACVA Initiator Concentration in the Feed on the Diameter D_n, Polydispersity PDI, and Iron Content in Magnetic PGMA Microspheres

Initiator	Conc. (wt %)	D_n (nm)	PDI	Fe (wt %)
APS	0.13	103	1.60	11.5
	0.20	100	2.18	8.6
	0.26	82	1.24	9.2
	0.33	78	1.21	9.4
ACVA	0.13	91	1.02	3.8
	0.20	79	1.03	4.5
	0.26	86	1.03	3.9
	0.33	88	1.02	3.9

Polymerization conditions: 0.75 wt % Disponil AES 60 in water; dextran-coated iron oxide/GMA, 0.33.

of iron were found in APS-initiated polymer microspheres than in those initiated with ACVA (Table II). This can be attributed to the sulfate anions present in the former particles which might facilitate stronger iron complexation than the carboxylates. The content of iron oxide in PGMA microspheres did not significantly depend on the initiator concentration.

Effect of emulsifier and its concentration

Three kinds of emulsifier were tested in the polymerization of GMA in the presence of dextran-coated iron oxide nanoparticles: anionic Disponil AES 60 and two nonionic surfactants used in cell biology—Tween 20 and Triton X-100. Poly(ethylene oxide)-based emulsifiers are known for their biocompatibility; they are even approved by FDA for some biomedical applications. A large effect of the emulsifiers was observed on morphology (sphericity, shape), size, and polydispersity of magnetic PGMA microparticles. According to SEM micrographs, superior magnetic PGMA microspheres with small size ($D_n = 84$ nm) and narrow size distribution (PDI = 1.04) were obtained with Disponil AES 60 [Fig. 6(a)]. In comparison with them, Tween 20 [Fig. 6(b)] and Triton X-100 surfactants [Fig. 6(c)] produced not strictly spherical and rather large polydisperse microparticles 360 nm (PDI = 1.28) and 427 nm (PDI = 1.22), respectively. The anionic charge of Disponil AES 60 obviously had a positive effect on emulsification. The effect of emulsifier concentration on the magnetic PGMA microsphere size and distribution was then investigated in more detail. The dependence

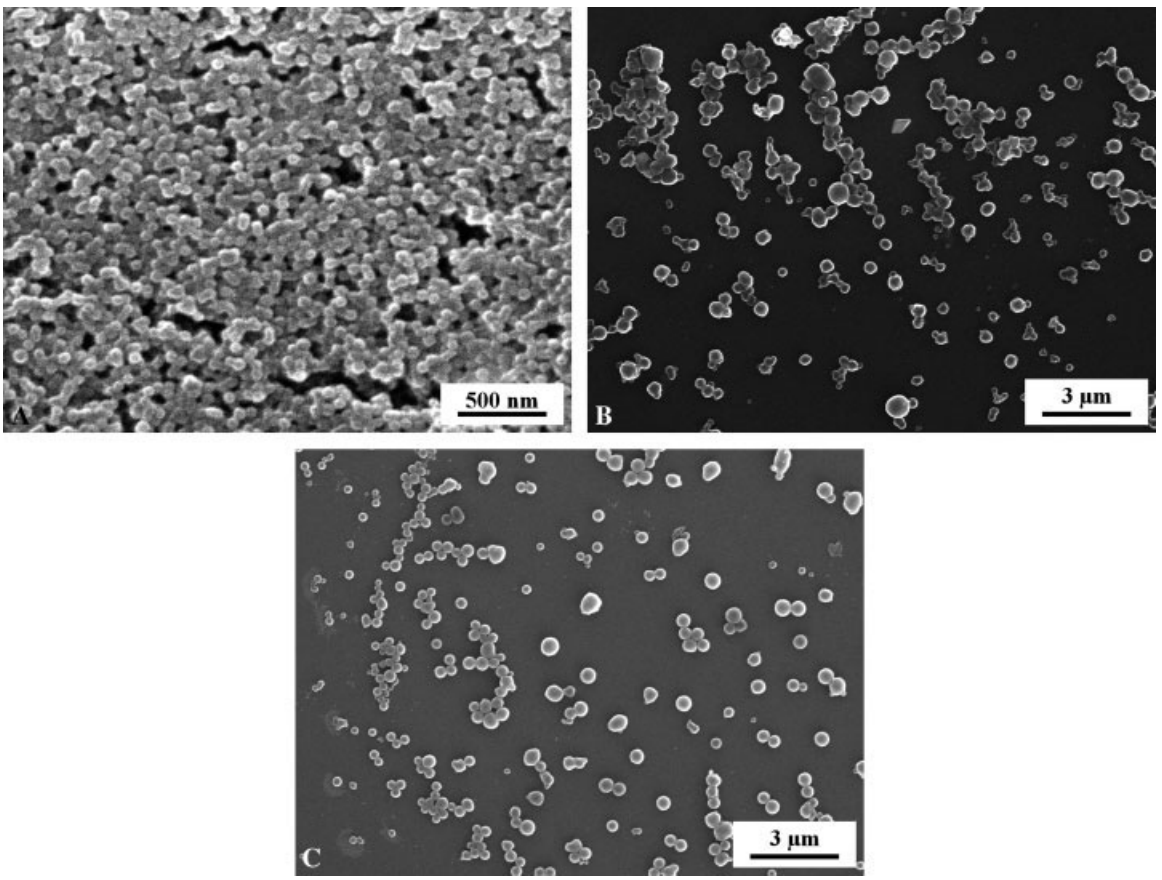

Figure 6 SEM of magnetic PGMA microspheres obtained by emulsion polymerization in the presence of 0.75 wt % of (a) Disponil AES 60, (b) Tween 20 and (c) Triton X-100 in water. Polymerization conditions: 0.26 wt % ACVA (relative to feed), dextran-coated iron oxide/GMA–0.33.

TABLE III
Effect of Triton X-100, Tween 20, and Disponil AES 60 Surfactant Concentration in Water on the Size D_n, Polydispersity PDI, and Iron Content in Magnetic PGMA Microspheres

Emulsifier	Conc. (wt %)	D_n (nm)	PDI	Fe (wt %)
Triton	0.15	313	1.20	2.0
	0.38	350	1.16	2.8
	0.75	427	1.21	1.4
	1.5	451	1.25	1.4
Disponil	0.15	122	1.34	1.7
	0.38	95	1.02	4.2
	0.75	86	1.03	3.9
	1.5	77	1.04	4.8
Tween 20	0.15	441	1.16	1.1
	0.38	344	1.20	0.7
	0.75	360	1.28	1.0
	1.5	356	1.93	1.3

Polymerization conditions: GMA – 15 wt % (relative to water), 0.26 wt % ACVA (relative to feed), dextran-coated iron oxide/GMA – 0.33.

of magnetic PGMA microsphere size on surfactant concentration in water confirmed that the particles produced with Tween 20 and Triton X-100 were substantially larger than those obtained with Disponil AES 60 (Table III). As expected, the particle size increased with decreasing concentration of Tween 20 (Table III) due to the reduced number of the micelles. A similar, but not too dramatic increase in the particle size was observed also with decreasing concentration of Disponil AES 60. The opposite trend was, however, found for Triton X-100. This can be explained in the context with the effect of the iron oxide present in the polymerization feed on the resulting PGMA particle size. The magnetic particle size is influenced not only by the emulsifier and its concentration, but also by the saccharide-coated iron oxide colloid. While with relatively hydrophobic Triton X-100 emulsifier, the particle size was larger in the nonmagnetic PGMA microspheres than in the magnetic ones, Disponil AES 60 and Tween 20 always produced smaller nonmagnetic microspheres than the magnetic ones (Figs. 4–6). This could mean that the effect of iron oxide colloid on the particle size prevails over the effect of the emulsifier at low Triton X-100 concentration decreasing thus the particle size. In contrast, the colloid does not much influence the magnetic particle size at high Triton X-100 concentrations. It is also interesting to note that the content of dextran-coated iron oxide incorporated in the microspheres increased with increasing concentration of Disponil AES 60 up to some 5 wt % of iron (Table III). This could be again ascribed to the solid complexation of sulfate anions of Disponil AES 60 with iron oxides, which increases with increasing emulsifier concentration. In contrast, a rather low content of incorporated iron oxide ($\sim$ 1–2 wt % Fe) was found in PGMA microspheres prepared using nonionic surfactants Tween 20 or Triton X-100 with the dextran-coated iron oxide/GMA ratio 0.33 documenting thus the importance of sulfate groups for preparation of magnetic microspheres (Table III).

Oxirane group content

Any micro- and nanoparticles are of no use if they do not have any reactive functional groups capable of attaching target biomolecules (enzymes, antibodies, drugs). The extraordinarily large surface area of emulsion nano/microparticles offers diverse opportunities of placing functional groups on the surface. It is a great advantage of PGMA microspheres, contrary to, e.g., styrene-based ones, that they can be easily modified in side chains by various reactions. Oxirane groups on a PGMA carrier can be easily hydrolyzed to vicinal diols, transformed to amines or aldehyde, $-SO_3^-$, $-N^{\oplus}R_3$, chelating and other functional groups.[31] Some authors, however, observed that the number of oxirane groups in the polymer does not correspond to the initial GMA because of their transformation during emulsion polymerization.[32] Also the presence of stabilizing hydrophilic poly(vinylpyrrolidone) anchored on polymer particles during dispersion polymerization could reduce the activity of oxirane groups on the particles.[33] In this report, concentration of Disponil AES 60 did not significantly affect the amount of oxirane groups ($\sim$ 7 mmol/g) at the constant iron oxide content in the feed (iron oxide/GMA = 0.33), as evidenced by IR spectroscopy. We have, however, observed the importance of the selection of proper polymerization initiator for the

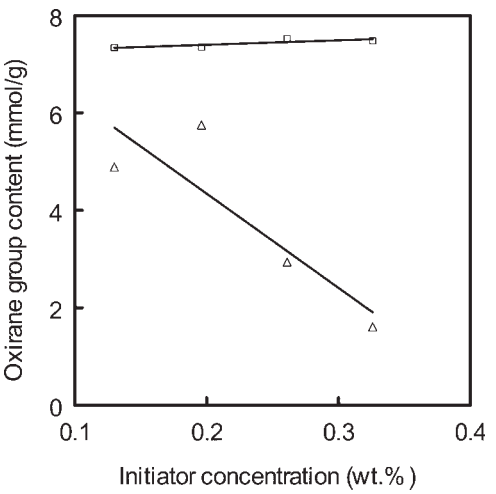

Figure 7 Effect of (□) ACVA and APS (△) initiator concentration in feed on the oxirane group content. Concentration of components: GMA 15 wt % (relative to water); dextran-coated iron oxide/GMA 0.33; Disponil AES 60 0.75 wt % (in water).

TABLE IV
Effect of Iron Oxide/GMA Weight Ratio in the Polymerization Feed on the Oxirane Group Content in Magnetic PGMA Microspheres

Initiator	Iron oxide/GMA (w/w)	Oxirane group Content (mmol/g)
ACVA	0	7.6
	0.11	7.3
	0.22	6.7
	0.33	6.6
	0.44	6.1
	0.53	5.4
APS	0	0
	0.11	0
	0.22	0
	0.33	2.2
	0.44	4.9

Polymerization conditions: CM-dextran-coated iron oxide, 1.5 wt % of Disponil AES 60 in water, 0.26 wt % of initiator in the feed.

oxirane group survival. While oxirane groups retained their reactivity after ACVA-initiated GMA polymerization and their content did not depend on the initiator concentration, the content of oxirane groups decreased with increasing APS concentration (Fig. 7) obviously due to their hydrolysis. Table IV then demonstrates the effect of the amount of iron oxide added to the polymerization feed on the content of oxirane groups in the microspheres depending on the selection of initiator. In ACVA-initiated system, increasing amount of iron oxide in the feed only slightly decreased the content of oxirane groups (Table IV). Persulfate-initiated system, however, produced particles without oxirane groups at the iron oxide/GMA weight ratio in the feed 0.22 and less, evidently due to their hydrolysis.[34] At the ratios higher than 0.22, some oxirane groups were already present in the polymer. This is in accordance with our previous observation, namely that the oxirane group content was reduced at high APS concentrations. We can then speculate that iron oxide interferes with APS and the negative effect of the initiator on oxirane group hydrolysis is thus partially alleviated at higher iron oxide/GMA ratios.

CONCLUSIONS

In summary, colloidal iron oxide nanoparticles can be prepared by precipitation of ferrous and ferric salts with ammonia in the presence of four saccharides: dextran, CM-dextran, DEAE-dextran, and D-mannose. The presence of mannose limited most the nanoparticle growth leading to very small values of particle size. Because the average particle size (estimated by TEM) of the iron oxide prepared in the present study was much less than the critical size of superparamagnetism[35] of magnetite (25 nm), the particles are superparamagnetic. A narrow magnetic PGMA particle size distribution was obtained by emulsion polymerization using moderate amounts of dextran- and CM-dextran-coated iron oxide core nanoparticles, Disponil AES 60 emulsifier and ACVA initiator. Dextran- and CM-dextran-coated iron oxide nanoparticles seemed to be well embedded in the polymer microspheres up to the iron oxide/GMA ratio 0.55. The microspheres show extensive potential applications for cheap and massive magnetic bioseparation, especially of proteins.

The authors thanks are due to Prof. Šňupárek of the University Pardubice for generous gift of Disponil AES 60 and Mrs. Hromádková for SEM measurements.

References

1. Audram, R. G.; Huguenard, A. P. U.S. Pat. 4,302,523 (1981).
2. Berry, C. C.; Curtis, A. S. G. J Phys D: Appl Phys 2003, 36, 198.
3. Elaissari, A.; Veyret, R.; Mandrand, B.; Chatterje, J. In Colloidal Biomolecules, Biomaterials, and Biomedical Applications; Elaissari, A., Ed.; Marcel Dekker: New York, 2003; p 1.
4. Tartaj, P.; Morales, M. P.; Veintemillas-Verdaguer, S.; Gonzáles-Carreno, T.; Serna, C. J. J Phys D: Appl Phys 2003, 36, 182.
5. Taupitz, M.; Schmitz, S.; Hamm, B. Fortschr Röntgenstr 2003, 175, 752.
6. Ellingsen, T.; Aune, O.; Berge, A.; Kilaas, L.; Schmid, R.; Stenstad, P.; Ugelstad, J.; Hagen, S.; Weng, E.; Johansen, L. Makromol Chem Macromol Symp 1993, 70/71, 315.
7. Molday, R. S.; MacKenzie, D. J Immunol Methods 1982, 52, 353.
8. Paul, K. G.; Frigo, T. B.; Groman, J. Y.; Groman, E. V. Bioconjugate Chem 2004, 15, 394.
9. Fan, J.; Lu, J.; Xu, R.; Jiang, R.; Gao, Y. J Colloid Interface Sci 2003, 266, 215.
10. Noguchi, H.; Yanase, N.; Uchida, Y.; Suzuta, T. J Appl Polym Sci 1993, 48, 1539.
11. Gilbert, R. G. In Emulsion Polymerization: A Mechanistic Approach; Academic Press: New York, 1995.
12. Ugelstad, J.; Kilaas, L.; Aune, O.; Bjorgum, J.; Herje, J.; Schmid, R.; Stenstad, P.; Berge, A. Advances in Biomagnetic Separation; Eaton: Natick, 1994; p 1.
13. Qui, G.; Wang, Q.; Wang, C.; Lau, W.; Guo, Y. Polym Int 2006, 55, 265.
14. Yang, C.; Guan, Y.; Xing, J.; Jia, G.; Liu, H. React Funct Polym 2006, 66, 267.
15. Elaissari, A. Macromol Symp 2005, 229, 47.
16. Huynh, R.; Chaubet, F.; Jozefonvicz, J. Angew Makromol Chem 1998, 254, 61.
17. Molday, R. S. U.S. Pat. 4,452,773 (1984).
18. Jolivet, J.-P.; Chaneac, C.; Tronc, E. Chem Commun 2004, 481.
19. Gupta, A. K.; Wells, S. IEEE Trans Nanobiosci 2004, 3, 66.
20. Arshady, R.; Pouliquen, D.; Halbreich, A.; Roger, J.; Pons, J. N.; Bacri, J. C.; Da Silva, M. F.; Hafeli, U. In Dendrimers, Assemblies, Nanocomposites; Arshady, R., Guyot, A., Eds.; Citus Books: London, 2002. The MML Series, Vol. 5.
21. Shafi, K. V. P. M.; Ulman, A.; Yan, X.; Yang, N.-L.; Estournes, C.; White, H.; Rafailovich, M. Langmuir 2001, 17, 5093.
22. Labský, J. Biomaterials 2003, 24, 4031.
23. Horák, D.; Semenyuk, N.; Lednický, F. J Polym Sci Polym Chem Ed 2003, 41, 1848.
24. Horák, D. J Polym Sci Polym Chem Ed 2001, 39, 3707.

25. Horák, D.; Boháček, J.; Šubrt, M. J Polym Sci Polym Chem Ed 2000, 38, 1161.
26. Horák, D.; Benedyk, N. J Polym Sci Polym Chem Ed 2004, 42, 5827.
27. Iwata, H.; Hata, Y.; Matsuda, T.; Taki, W.; Yonekawa, Y.; Ikada, Y. Biomaterials 1992, 13, 891.
28. Li, P.; Yu, B.; Wei, X. J Appl Polym Sci 2004, 93, 894.
29. Fitch, R. M.; Tsai, C. H. In Polymer Colloids; Fitch, R. M., Ed.; Plenum Press: New York, 1971; p 73.
30. De Winter, W.; Zimmermann, D.; Declerq, R. In Macromolecular Engineering. Recent Advances; Mishra, M. K.; Nuyken, O.; Kobayashi, S.; Yagci, Y.; Sar, B., Eds.; Plenum Press: New York, 1995; p 229.
31. May, A. C., Ed. Epoxy Resins: Chemistry and Technology; Marcel Dekker: New York, 1988.
32. Žůrková, E.; Bouchal, K.; Zdeňková, D.; Pelzbauer, Z.; Švec, F.; Kálal, J. J Polym Sci Polym Chem Ed 1983, 21, 2949.
33. Chen, C.-H.; Lee, W.-C. J Chromatogr A 2001, 921, 31.
34. Eliseeva, V. I. Polymer Dispersions (in Russian); Khimiya: Moscow, 1980; p 295.
35. Lee, J.; Isobe, T.; Senna, M. J Colloid Interface Sci 1996, 212, 490.